Desalination and Water Treatment
www.deswater.com
doi: 10.5004/dwt.2020.26305

206 (2020) 315–330
December

Synthesis, characterization, and tetracycline adsorption behavior of activated carbon dopped alginate beads: isotherms, kinetics, thermodynamic, and adsorption mechanism

Fulya Korkut[a], Didem Saloglu[b,*]

[a]*Department of Chemical and Process Engineering, Institute of Science, Yalova University, Yalova, Turkey, Tel. +90 2268155904; Fax: +90 2268155392; email: fulya.korkut@yalova.edu.tr (F. Korkut)*
[b]*Chemical Engineering Department, Faculty of Engineering, Yalova University, Yalova, Turkey, Tel./Fax: +90 2268155392; email: didemsalogludertli@gmail.com (D. Saloglu)*

Received 12 February 2020; Accepted 27 June 2020

ABSTRACT

The main aim of the current work is to test the tetracycline adsorption behavior of activated carbon (AC) dopped alginate (ALG) beads. In this way, synthesis and characterization of activated carbon dopped alginate beads using Fourier-transform infrared, thermogravimetric analysis, differential scanning calorimetry, scanning electron microscopy, Brunauer–Emmett–Teller, X-ray photoelectron spectroscopy analysis, adsorption equilibrium, kinetics, thermodynamics, adsorption mechanism, desorption, and reusability experiments were carried out. Maximum tetracycline removal percentage was achieved using 200 mg of AC-ALG beads with a ratio of 3.0% (w/v) within 6 h at pH 7.0, and tetracycline removal performance was determined to be 100.0%. The Langmuir, Freundlich, Dubinin–Radushkevich, Temkin, Halsey, and Harkins–Jura isotherm models were applied to experimental data. AC-ALG-(1.0 and 2.0) beads were found to fit the Langmuir model well, while AC-ALG-3.0 beads fitted the Freundlich model. Adsorption kinetics were investigated by pseudo-first-order, pseudo-second-order, Elovich, Weber–Morris intraparticle diffusion, and Bangham models and the pseudo-second-order kinetic model fitted the adsorption data well. The thermodynamic parameters were calculated, and the enthalpy of tetracycline adsorption was endothermic for all beads. After the adsorption process, the beads can easily be regenerated by NaOH and effectively reused within five cycles. It can be concluded that activated carbon dopped alginate beads have a considerable potential on the adsorption of pharmaceutical compounds from wastewater.

Keywords: Activated carbon; Alginate; Tetracycline; Adsorption; Mechanism

1. Introduction

Antibiotics, also known as antibacterials, are a group of medicines that are used to treat the infections caused by bacteria and parasites. The usage of antibiotics to treat human diseases and infections and to promote growth in livestock increase every year. Because of this increased use in antibiotics, several studies have indicated the presence of antibiotic residues in water sources including surface water, groundwater, domestic water, municipal water, wastewater, and industrial effluents [1].

The most-often detected antibiotics in various water sources are penicillin, amoxicillin, azithromycin, ciprofloxacin, sulfamethoxazole, and tetracyclines. Among them, tetracycline is a broad-spectrum polyketide antibiotic; it is the second most widely used in the world and has medical and veterinary applications. Very low amounts of tetracycline administered to the treated humans and animals are

* Corresponding author.

metabolized in the body, with most of the unmetabolized form of the antibiotic being eliminated with urine. Residues of tetracyclines are frequently detected in surface water, wastewater, groundwater, and domestic water. Tetracycline groups of antibiotics exist in the range of 1.2–4.0 μg L^{-1} levels in wastewater and domestic water. Tetracycline at μg L^{-1} levels in wastewater has the potential to cause negative health effects, and removal of the drug from wastewater is an important subject for researchers [2].

Removing tetracycline from wastewater is studied using photocatalysis, redox reactions, and electron pulse irradiation, but these methods are not convenient for practical separation techniques. Among practical separation techniques, adsorption is one of the methods that can be used for removing tetracycline from the wastewater; it is a low cost, easily operated, and has a high removing rate [3]. Adsorption of tetracycline can be investigated using carbonaceous adsorbents such as activated carbon, carbon fiber, carbon nanotubes, etc. due to their high surface areas and pore size distributions. Furthermore, considering environmental concerns, various biopolymers have attracted great interest for use as an adsorbent in wastewater treatment. In the last decade, carbon-containing biopolymers with high adsorption capacity and adsorption rates have considerable potential for adsorption [4]. One biopolymer, alginate, is a natural, linear polysaccharide that has been applied in a variety of micropollutants such as pharmaceuticals, food, and dyes [5,6]. Therefore, introducing activated carbon into the raw alginate's molecule significantly increases the surface area of the raw alginate molecule [7] and improves the adsorption rate; meanwhile, a new and innovative adsorbent can be designed for the adsorption of tetracycline from wastewater.

The objective of the present paper is to evaluate the adsorption capacity of the alginate beads for the removal of tetracycline from wastewater after the dopping activated carbon. In the present study, physicochemical and morphological properties of the activated carbon dopped alginate beads (AC-ALG) were characterized, and the effects of various parameters, such as pH, amount of adsorbent, temperature, and time were analyzed for adsorption of tetracycline. The Langmuir, Freundlich, Temkin, Dubinin–Radushkevich (D–R), Halsey, and Harkins–Jura adsorption isotherm models and pseudo-first-order, pseudo-second-order, Elovich, Weber–Morris, and Bangham kinetics models were studied. The thermodynamic parameters such as enthalpy, entropy, and Gibbs free energy, adsorption mechanism, desorption, and reusability experiments were also carried out. It can be stated that this work represents the first example in the literature to follow synthesis, characterization, and adsorption behavior of AC-ALG beads for tetracycline.

2. Materials and methods

2.1. Materials

Sodium alginate was purchased from Acros Organics (Belgium); tetracycline, NaCl, and $CaCl_2$ were produced by Sigma-Aldrich (Germany); ethanol, HCl, and NaOH were supplied by Merck (Germany). Activated carbon with 850 m^2 g^{-1} surface area, micropore volume 0.22 cm^3 g^{-1}, and mesopore volume 0.44 cm^3 g^{-1} was obtained from Zag Chemicals (Turkey). All reagents were of analytical-grade chemicals and used as received.

2.2. Preparation of alginate beads

2% (w/v) of sodium alginate solution was prepared in 0.1 M NaCl solution. The alginate solution was added dropwise to 0.1 M $CaCl_2$ solution using a plastic syringe and left with a magnetic stirrer for 24 h at 25°C. The obtained calcium alginate wet beads were detached gently from the medium and washed using distilled water. Finally, these beads were dried in an oven at 60°C for 24 h and codded to be ALG beads [5,8,9].

2.3. Preparation of activated carbon dopped alginate beads

To synthesize activated carbon dopped alginate (AC-ALG) beads, alginate was dissolved in 0.1 M NaCl solution with continuous stirring to have a final concentration of 1.0% (w/v). Activated carbon was added to ALG solution with different AC:ALG ratios of 1.0–3.0 (w/v). The preparation, purification, and drying of the beads were the same as described in the preparation of raw ALG beads. The beads were codded to be AC-ALG-(1.0–3.0) [5,8,9].

2.4. Characterization of beads

Raw ALG and AC-ALG beads were investigated by IR affinity spectrometer (Perkin Elmer, Turkey) using the KBr pellet technique [7]. Thermal characterizations of the beads were carried out by thermogravimetric analysis (TG, Perkin Elmer, Turkey), and differential scanning calorimetry (Diamond DSC, Turkey) from 20°C to 800°C at 10°C min^{-1} heating rate. The surface morphologies of the beads were observed by scanning electron microscopy (SEM, Philips XL-30, United States), and Brunauer–Emmett–Teller (BET) analysis was performed using a surface analyzer (ASAP 2020, France) [8]. The points of zero charges (PZC) of ALG, AC, and AC-ALG beads were established using salt addition method [9].

2.5. Preliminary adsorption experiments

In batch adsorption experiments, 25 mL of 20 mg L^{-1} tetracycline solution with pH from 4.0 to 10.0 was added to 20–200 mg of AC, ALG, and AC-ALG-(1.0–3.0) in a 50 mL Erlenmeyer at 25°C ± 0.5°C. Adsorption experiments were performed utilizing a shaker at 140 rpm for 6 h. Then the beads were separated from the solution, and the residual concentrations of the tetracycline in the supernatant were monitored spectrophotometrically with a double-beam spectrophotometer at 360 nm. Adsorption experiments were repeated three times; the standard deviations were within ca. ±5%, and all results are reproducible [8,9].

Adsorption isotherm experiments were conducted by utilizing 20 mg L^{-1} tetracycline solution at pH 7.0 using 20–200 mg of AC, ALG, and AC-ALG-(1.0–3.0) beads in a 50 mL Erlenmeyer flask at 25°C ± 0.5°C for 6 h. The amount of tetracycline adsorbed onto the beads at equilibrium [8,9], q_e (mg g^{-1}) was calculated by the following expression:

$$q_e = \frac{(C_i - C_e)}{m} V \quad (1)$$

Adsorption isotherms of tetracycline onto AC, ALG, and AC-ALG-(1.0–3.0) beads were described with the Langmuir, Freundlich, D–R, Temkin, Halsey, and Harkins–Jura models. Similarly, adsorption kinetics experiments were carried out using 20 mg L^{-1} tetracycline solution at pH 7.0 using 200 mg of ALG and AC-ALG-(1.0–3.0) beads for interval times, and the adsorption kinetics were investigated by pseudo-first-order, pseudo-second-order, Elovich, Weber–Morris, and Bangham models [6,8]. The adsorption experiments were carried out for 25°C, 45°C, and 60°C ± 0.5°C at pH 7.0, tetracycline concentration 20 mg L^{-1}, and contact time 6 h to determine the adsorption thermodynamic parameters [9].

2.6. Desorption and reusability

Desorption studies were performed by suspending tetracycline-loaded AC-ALG-3.0 beads in 3 M NaOH, 1 M HCl, and ethanol. Firstly, 200 mg of beads were added to 20 mg L^{-1} tetracycline solutions. Then, tetracycline-loaded beads and NaOH, HCl, and ethanol were separately shaken for 6 h, and residual tetracycline concentration was measured spectrophotometrically. Desorption efficiency was calculated as the ratio of desorbed to the adsorbed amount of tetracycline [9,10].

Ten cycles of consecutive adsorption–desorption studies in 3 M NaOH were performed in order to check the reusability of regenerated AC-ALG-3.0 beads. The beads were added to 20 mg L^{-1} tetracycline solution, and the obtained suspension was shaken at room temperature for 6 h. Subsequently, the suspension was filtered, and the tetracycline concentration was measured spectrophotometrically. After adsorption, tetracycline-loaded AC-ALG-3.0 beads were collected, dried, and then used for the desorption experiment. The collected beads were added to 50 mL NaOH, and the suspension was shaken at room temperature for 6 h. Then the suspension was filtered, and the concentration of tetracycline was measured again [9,10].

3. Results and discussion

3.1. Characterization of beads

FT-IR analysis was performed to examine the functional groups on AC, ALG, and AC-ALG-(1.0–3.0) beads in the range of 650 and 4,000 cm^{-1} (Fig. 1). The spectra of AC represent the peaks near 4,000; 2,850; and 2,450 cm^{-1} attribute O–H, C–H stretching (from CH_2), and C–H stretching (from CH_3), respectively. The sharp peak near 2,300 cm^{-1} corresponds to C–O bonds. Another relatively broad peak near 2,100 cm^{-1} attributes to the allene (C=C=C) group. The band near 1,700 cm^{-1} represents the C=O stretching of carboxyl groups. The broadband near 1,000 cm^{-1} illustrates the oxidized carbons and has been assigned to C–O stretching in acids [8]. The FT-IR spectrum of ALG beads indicates a number of absorption peaks (Fig. 1). The absorption peak near 3,300 and 2,950 cm^{-1} attributes to O–H and C–H groups of alginate. The characteristic peaks at 1,610 and 1,450

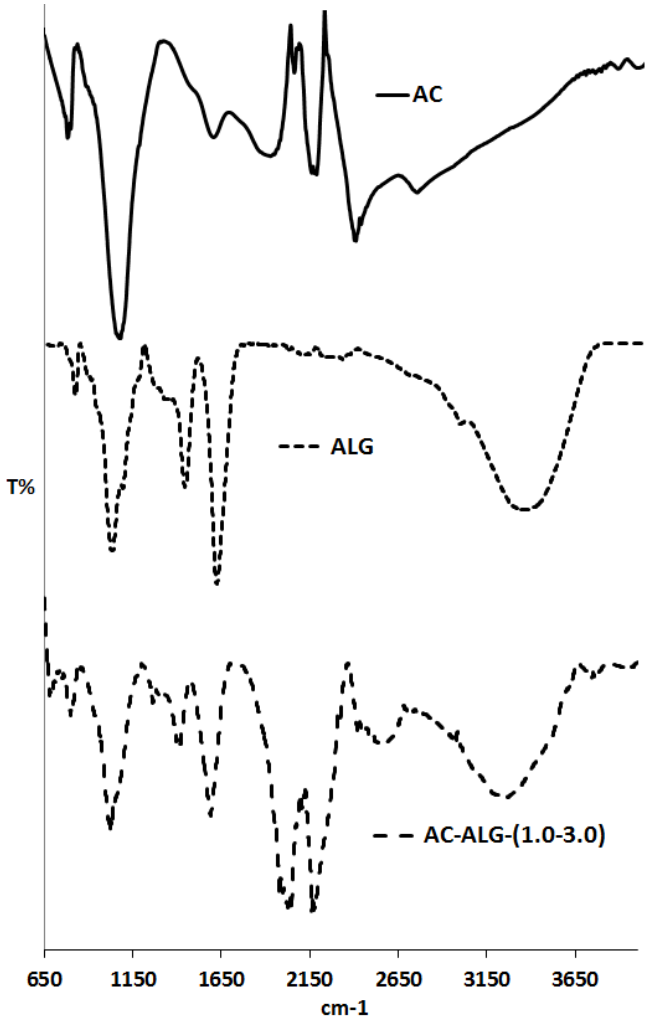

Fig. 1. FT-IR spectra of AC, ALG, and AC-ALG beads.

represent the stretching of C–O–O (asymmetric) and C–O–O (symmetric) bonds, respectively. The bands around 1,095; 1,075; and 1,035 cm^{-1} attribute to C–O, C–C, and C–C bending vibration of raw alginate beads [11]. According to these results, AC-ALG beads showed significant difference bands in comparison with AC and raw ALG beads. Absorption region of stretching vibration of O–H and asymmetric and symmetric C–O–O bonds in AC-ALG beads appeared significantly lower intensity than raw ALG. These differences resulted from the participation of O–H and C–O–O groups of alginate to the activated carbon in order to chelating structure. The change in the bands is evidence of interaction between AC and ALG, and it can be safely mentioned that AC-ALG beads were synthesized successfully.

The thermal stabilities of ALG and AC-ALG-(1.0–3.0) beads were characterized by TGA (Fig. 2a). As can be seen from the TGA trace, in the temperature range of 25°C–800°C, all AC-ALG beads are degraded at a slower rate than raw ALG. AC-ALG beads displayed retardation of the thermal degradation above 60°C. The char yield of all AC-ALG beads was found to be higher than that of raw ALG. Although ALG was not thermally stable when the temperature was

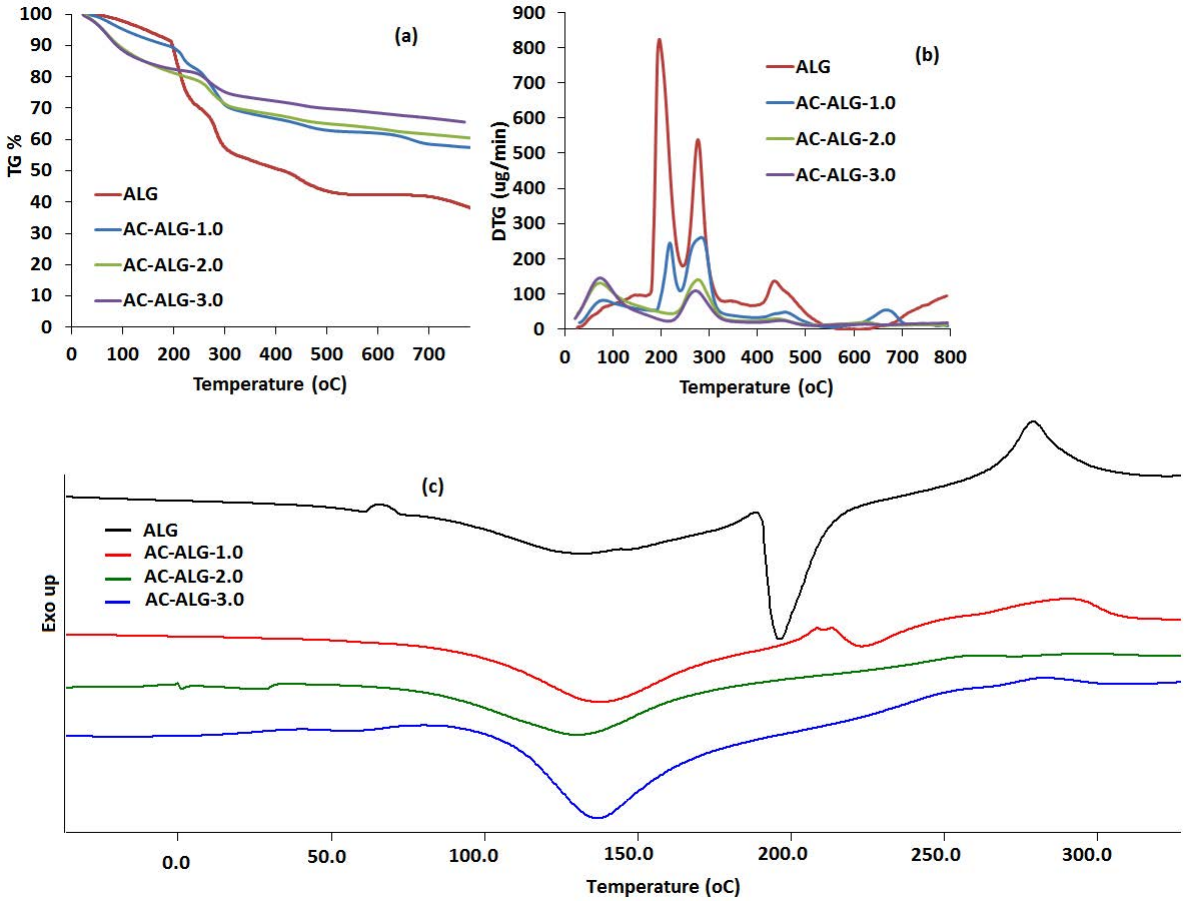

Fig. 2. TGA thermograms of ALG and AC-ALG beads (a), their derivative curves of weight loss (b), and DSC curves of ALG and AC-ALG beads (c).

increased, 60% of the beads decomposed before 500°C, and nearly 40% decomposed between 25°C and 300°C. The char yield ratios were found as 40%, 57%, 60%, and 65% for ALG, AC-ALG-1.0, AC-ALG-2.0, and AC-ALG-3.0 beads, respectively [11,12]. As can be seen from the DTG curves (Fig. 2b), AC-ALG-(1.0–3.0) beads had lower degradation rates at their maximum weight loss in the temperature range of 25°C–800°C. The highest residue as well as the lowest degradation rate was achieved for AC-ALG-3.0 beads. The highest thermal stability might be ascribed to the interaction between AC and ALG beads due to high AC content, and it is mentioned that the contribution of AC to raw alginate beads decreased the molecular flexibility of the AC-ALG polymer chains. As can be seen from Fig. 2b, raw ALG beads degraded with a higher rate in the temperature range of 25°C–800°C compared with all AC-ALG beads. Three degradation phases were detected for raw ALG beads at near 200°C, 250°C, and 450°C. The weight loss is probably due to the removal of water and the degradation of the end-chain groups of the ALG matrix. Also, Fig. 2b shows four degradation phases for AC-ALG-1.0 beads. The first phase was in the range of 180°C–230°C, the second phase was between 230°C and 310°C, the third phase was about 400°C–500°C, and the last phase was between 600°C and 700°C. Moreover, three degradation phases were detected for AC-ALG-2.0 and AC-ALG-3.0 beads. The first phase was near 100°C, the second phase was between 250°C and 320°C, and the third phase was about 400°C–480°C. From the comparison of DTG curves of all AC dopped beads, it is clear that the first and second decomposition phases resulted from the thermal degradation of raw ALG molecules; AC-ALG beads have a lower degradation rate. Furthermore, raw ALG had 5.2 and 3.4 times higher degradation rate than AC-ALG-3.0 and AC-ALG-1.0 beads. The AC-ALG beads had higher thermal stability with a higher char yield than that of raw ALG beads. This improvement in thermal stability can be ascribed to the interaction between ALG and AC interactions and the restriction of molecular mobility of the polymer chains [11,12].

DSC analyses of raw ALG and AC-ALG-(1.0–3.0) beads were performed between –80°C and 350°C under the nitrogen atmosphere (Fig. 2c). Two endothermic peaks between 120°C and 180°C followed by an exothermic peak at nearly 300°C were determined for ALG beads. The first endothermic region (near 120°C) was due to the separation of moisture associated with the hydrophilic groups of the alginate. The second endothermic region (near 180°C) represented the melting point of ALG beads. The thermogram of the beads showed an exothermic peak at about 300°C, which attributed its decomposition. As shown in Fig. 2c,

AC-ALG-1.0 beads showed two different melting peaks at around 120° and 220°C. So, the related peaks may be attributed to the melting of the polymer crystals having interactions with AC. Also, DSC curves of AC-ALG-(2.0–3.0) beads had some differences in the melting region of the others. They showed only one melting peak at around 120°C, and this can be explained due to the high AC content changing the chain arrangement of the alginate molecules. The peaks were much clearer in Fig. 2c thermogram of AC-ALG-3.0 involving the highest amount of AC [11,12].

The SEM images of AC, ALG, and AC-ALG-(1.0–3.0) beads are given in Fig. 3. As can be seen from the figure, ALG surface was very rough and full of long cracks and microfractures. It is obvious that numerous microfractures (ca. 500 μm) on the surface of ALG were determined, and the microfractures fully covered the surface of the beads and supplied a uniform area. This surface morphology made ALG very suitable for AC dopping into the microfractures and cracks (Figs. 3a and b). It seems clear that, the surfaces of ALG beads changed distinctively after modification with AC, having a three-dimensional network structure (Fig. 3c) and resulted in a surface with smaller cracks and cavities. With increasing AC content in the alginate, the length of cavities decreased from nearly 500 to 50 μm, and the beads were coated by non-uniform cavities. The AC-ALG beads were found to have greater numbers of shorter microfractures (ca. 20–50 μm) together with the presence of cavities. The existence of a similar surface has been described for all beads, and this morphology occurred by decorating surface cavities by dopping AC. According to the high-magnification SEM images, AC-ALG-(1.0–3.0) beads have a subporous structure (Figs. 3d and e). The beads did not show a porous structure in the weak-magnitude SEM image, but very narrow pores/cavities (ca. 20–50 μm) occurred in high magnification of the SEM images. Also, as represented in the figure, when focused on the beads' surface, a number of narrow rooms and cavities, the cavity in cavities, and microfractures were seen. Microfractures and cavities covering the entire surface of the AC-ALG beads and providing a uniform area were foreseen to be the result of the formation of sub-networks. The SEM images can be accepted as an indication of dopping AC into alginate. The presence of cavities and cracks on the AC-ALG surface can be said to be necessary for tetracycline adsorption.

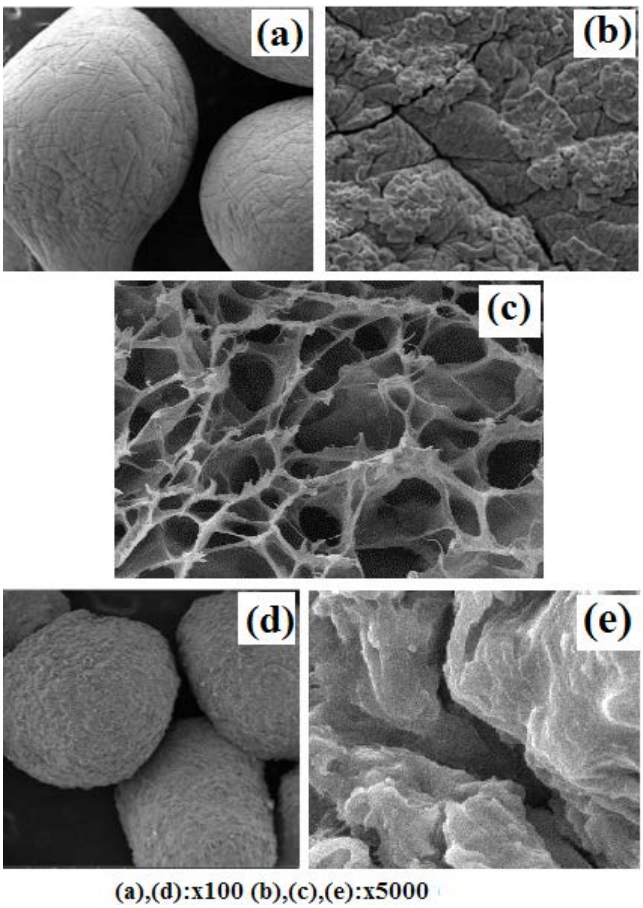

Fig. 3. SEM images of surfaces of ALG beads ((a and b) low and high magnifications), AC ((c) high magnification), and AC-ALG beads ((d and e) low and high magnifications).

The results obtained from SEM analysis were also supported by BET analysis. The specific surface areas of AC, ALG, and AC-ALG-(1.0–3.0) were recorded as AC > AC-ALG-3.0 > AC-ALG-2.0 > AC-ALG-1.0. Also, total pore volumes were raised by introducing AC into ALG. AC represented the largest total pore volume; therefore, larger pores were formed on the AC-ALG beads. The total pore volume values were found as 0.158, 0.214, and 0.278 $cm^3 g^{-1}$ for AC-ALG-1.0, AC-ALG-2.0, and AC-ALG-3.0, respectively. The restoration of the surface properties of ALG existed by AC part of a performance as a supporting material [12].

3.2. Preliminary adsorption experiments

The effect of the amount of adsorbent on the tetracycline adsorption was investigated in the range of 20–200 mg of AC, ALG, and AC-ALG-(1.0–3.0) for 20 mg L^{-1} tetracycline solution (Fig. 4a). The tetracycline removal % values increased from 48% to 100% for AC; 14% to 34% for ALG beads; from 36% to 86% for AC-ALG-1.0; from 34% to 92% for AC-ALG-2.0; and from 37% to 100% for AC-ALG-3.0 as the amount of adsorbent increased from 20 to 200 mg g^{-1}. Removal % values of tetracycline were found to be 20%, 100%, 42%, 72%, and 88% using 100 mg of ALG, AC, AC-ALG-1.0, AC-ALG-2.0, and AC-ALG-3.0, respectively. Also, as the amount of beads increased from 100 to 200 mg, tetracycline adsorption removal % values boosted effectively and were determined to be 20%, 86%, 92%, and 100% using ALG, AC-ALG-1.0, AC-ALG-2.0, and AC-ALG-3.0, respectively. Thus, 3.0% (w/v) AC content in the raw ALG beads was used as the optimum activated carbon content for tetracycline adsorption. Maximum tetracycline removal % was determined to be 100% for 200 mg of AC-ALG-3.0 and AC within 6 h at pH 7.0. The increment in the tetracycline removal percentages with the amount of the beads was attributed to the enhancement of the beads' surface area and the availability of more adsorption active sites. Hence, 200 mg of adsorbent was selected as the optimum amount of adsorbent, and 200 mg of AC-ALG-3.0 was applied for following the pH effect on the adsorption experiments.

Fig. 4b shows the surface charge of AC, ALG, and AC-ALG beads. ALG beads had a positive surface charge at

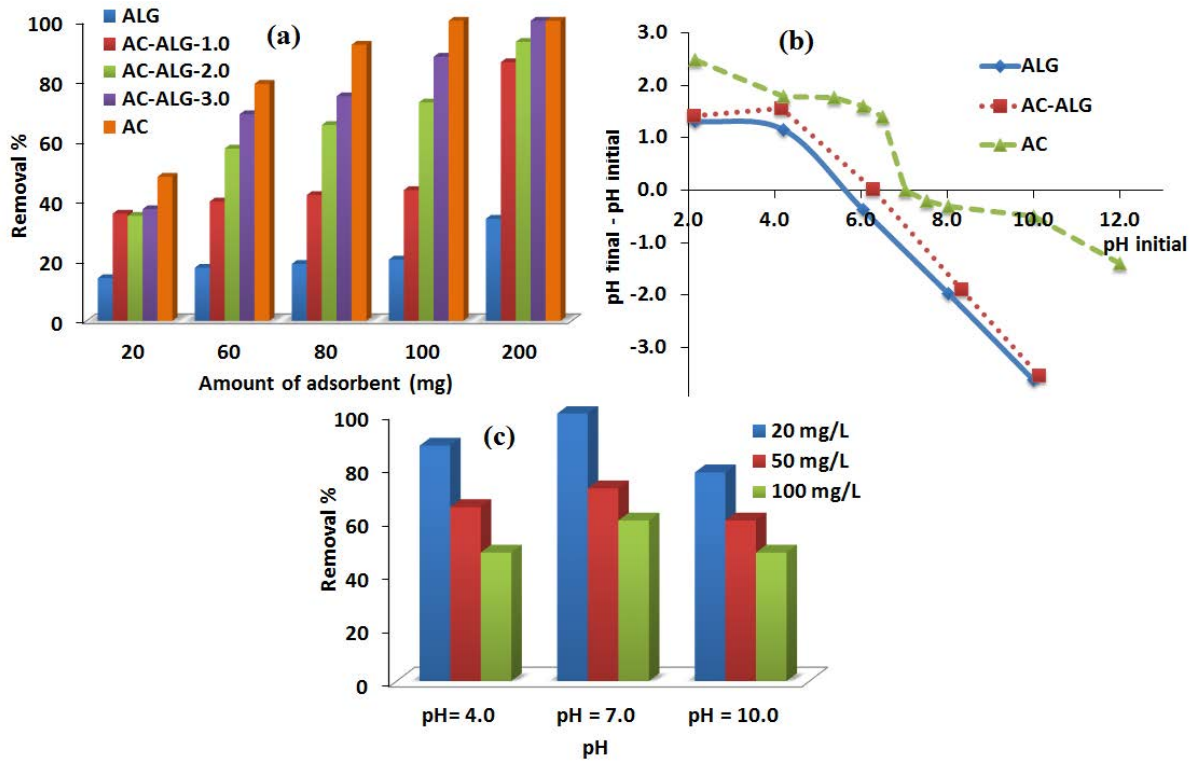

Fig. 4. Effect of adsorbent amount on the removal % of tetracycline onto AC, ALG, and AC-ALG beads (a), surface charge of AC, ALG, and AC-ALG beads (b), and effect of pH on the removal % of tetracycline onto of AC-ALG-3.0 beads (c).

pH lower than 5.6 owing to the presence of –COOH groups of the polymer and point of zero charges of AC-ALG beads was recorded as pH 6.3. When compared with raw ALG beads, the PZC values of AC-ALG beads were increased after dopping AC due to the deprotonated carboxylic acids of alginate. The PZC values of AC-ALG beads showed that when the pH ranged from 6.3 to 12.0, the surface of the beads was negatively charged, and when pH was below 6.3, the surface was positively charged. On the other hand, the pH of the tetracycline solution changed charges of the groups of chemicals on it. Tetracycline transforms a cationic molecule by protonation of NH groups at the pH below 3.3; also it carries both positive and a negative charge groups (dimethyl-ammonium and phenolic diketone) when pH value is between 3.3 and 7.7, and the antibiotic converts an anionic molecule by deprotonation of carbonyl groups at pH higher than 7.7 [13]. Therefore, when pH was between 6.3 and 7.7, both protonated and deprotonated tetracycline groups in the solution and the surface of AC-ALG beads were negative, so the cationic groups of the tetracycline can be adsorbed on AC-ALG beads, and it was beneficial for ion exchange between the antibiotic and the beads. At pH 7.0 (>$PZC_{AC\text{-}ALG}$), AC-ALG bead surfaces were deprotonated; thus, a negative charge was formed on the surface, hydrogen bonds occurred between –OH and –COOH groups of AC-ALG beads and protonated phenolic diketone groups of the tetracycline and adsorption efficiency increased significantly. Furthermore, a similar trend can be seen at pH 4.0. However, when pH was above 7.7, anionic groups were the main species of the tetracycline solution, and the surface of AC-ALG was still negative. Thus, the antibiotic cannot be effectively adsorbed on the AC-ALG beads due to the electrostatic repulsion. Therefore, the adsorption of tetracycline onto AC-ALG beads may be due to the hydrogen bonding, electrostatic repulsion, Van der Waals forces [13].

Tetracycline solutions at pH 4.0, 7.0, and 10.0 were prepared in order to determine the effect of pH on the adsorption capacity of the beads using initial tetracycline concentration of 20, 50, and 100 mg L^{-1} (Fig. 4c). From Fig. 4, it can be seen that the removal efficiency of tetracycline was 100% at pH 7.0 for 20 mg L^{-1} tetracycline solution. However, the adsorption rate of tetracycline decreased from 100% to 88% and 78% when pH decreased from 7.0 to 4.0 and 10.0. Furthermore, there was a similar behavior for 50 and 100 mg L^{-1} tetracycline solutions. Thus, the removal of tetracycline using AC-ALG-3.0 beads was very efficient at neutral pH value. Fig. 4c also shows the effect of tetracycline solution concentration on adsorption. It was found that the tetracycline removal percentages decreased from 100% to 72% and 60%, respectively, with an increase in tetracycline concentrations from 20 to 50 and 100 mg L^{-1} at pH 7.0. In addition to this, the removal percentages decreased from 78% to 60% and 48% in a tetracycline concentration range between 20 and 100 mg L^{-1} at pH 10.0, and the adsorption removal percentages showed a similar downward trend at pH 4.0. It is attributed to the saturation of adsorption sites of the beads. Saturation of the sites of the beads is a case in which adsorbed phase volume is totally filled with tetracycline. Therefore, active sites of the AC-ALG-3.0 beads were totally filled and closed with tetracycline molecules at

20 mg L^{-1} solution concentration, so adsorption efficiency significantly decreased with an increasing concentration [13].

3.3. Adsorption isotherms

The first step for adsorption research is to identify an appropriate type of adsorption curves. For the classification of adsorption curves, the two most common methods being used are Brunauer's five types of adsorption curves and Giles types of adsorption curves [14]. Type III isotherms according to Brunauer classification were obtained for ALG and AC-ALG-(1.0–2.0) beads. The Type III model represents the adsorption process on an adsorbent with big pores, and the interaction between adsorbate and adsorbent surface is weaker. Moreover, the Type II isotherm was shown for AC and AC-ALG-3.0. Type II isotherm is obtained by adsorbents with big pores with the strong interaction of the adsorbent and adsorbate. On the other hand, initial slopes of the graphs showed that S and H types according to the Giles classification were obtained for ALG and AC-ALG-(1.0–2.0) beads; AC and AC-ALG-3.0 beads, respectively. It is reported that S and H types represent the Langmuir model and high affinity of the adsorbent and adsorbate molecules, respectively. Therefore, H type indicates a good affinity of the AC-ALG-3.0 beads for tetracycline [14].

The correlation between C_e and q_e values was characterized by the following models: Langmuir, Freundlich, D–R, Temkin, Halsey, and Harkins–Jura. Equilibrium adsorption isotherms of tetracycline using AC, ALG, and AC-ALG-(1.0–3.0) beads are shown in Fig. 5. The related

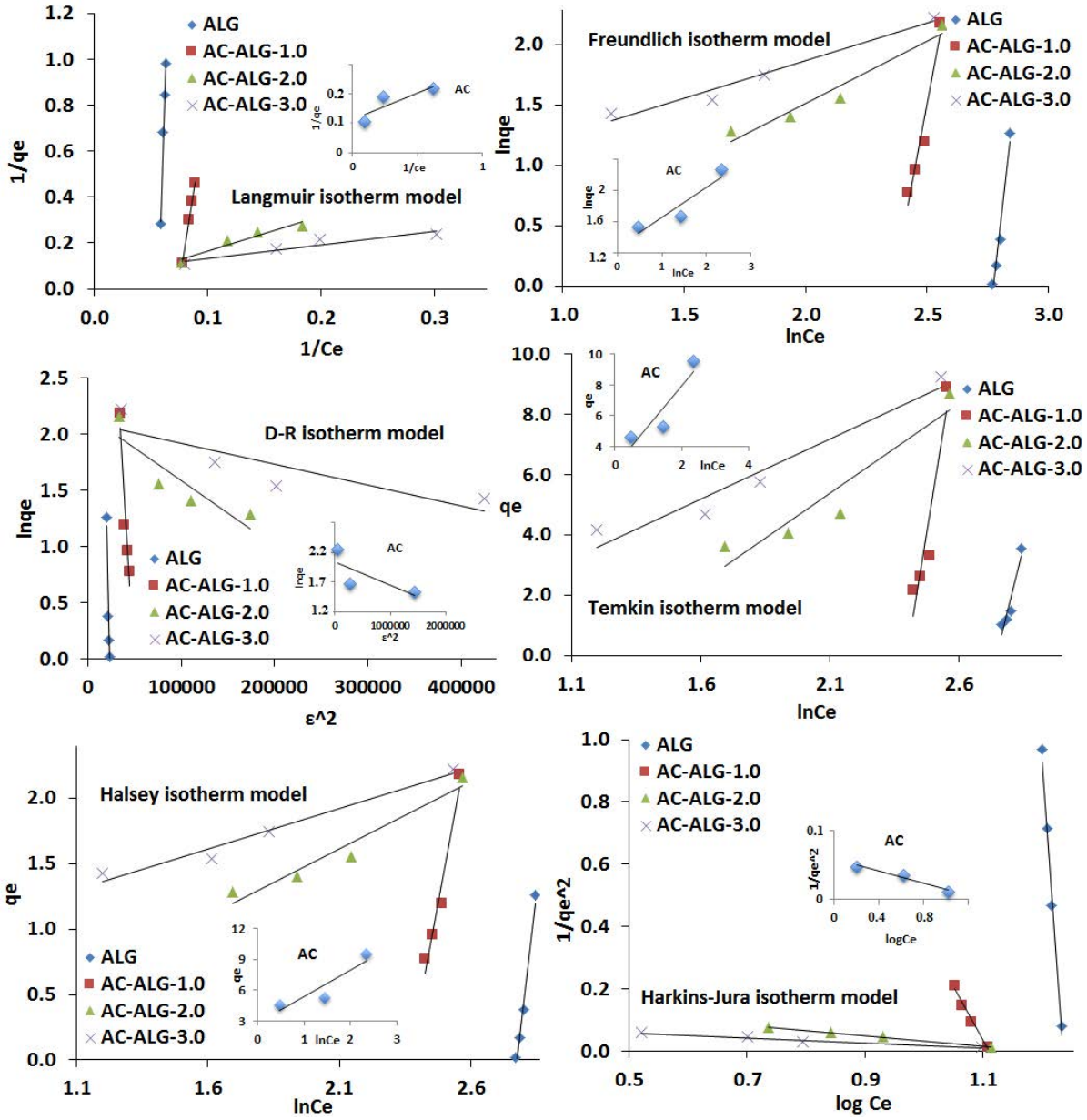

Fig. 5. Adsorption isotherm models of tetracycline onto AC, ALG, and AC-ALG beads.

model parameters were obtained from the slope and intercept of the linearized isotherm plots [15,16]. Table 1 represents the adsorption isotherm parameters and correlation coefficients (R^2) of tetracycline adsorption onto AC, ALG, and AC-ALG beads. Furthermore, Fig. S1 and Table S1 show a comparison of the isotherm model capacities and R^2 and Chi-square values (χ^2) of AC-ALG-3.0 beads using a non-linear approach [15].

The Langmuir isotherm model is based on monolayer coverage and homogeneous active sites of the adsorbents. The adsorbents are structurally homogeneous, and active sites on the adsorbents are energetically equivalent. The model is defined as Eq. (2):

$$\frac{1}{q_e} = \frac{1}{q_m K_L}\frac{1}{C_e} + \frac{1}{q_m} \tag{2}$$

where q_m (mg g^{-1}) and K_L are model parameters related to monolayer adsorption capacity and free adsorption energy constant, respectively [15]. q_m values were calculated to be 8.4 mg g^{-1} for AC; 0.1 mg g^{-1} for ALG; 0.4 mg g^{-1} for AC-ALG-1.0; 62.5 mg g^{-1} for AC-ALG-2.0; and 13.7 mg g^{-1} for AC-ALG-3.0, respectively (Table 1). Furthermore, K_L values were determined to be 0.64, 0.05, 0.07, 0.01, and 0.12 L mg^{-1} for AC, ALG, and AC-ALG-(1.0–3.0), respectively. R_L (equal to $(1/(1 + C_e K_L))$ values were calculated to be 0.072 for AC; 0.5 for ALG; 0.42 for AC-ALG-1.0; 0.83 for AC-ALG-2.0; and 0.29 for AC-ALG-3.0. R_L values for all beads were calculated between 0.0 and 1.0, and it can be concluded that tetracycline adsorption was favorable. The linear regression coefficient (R^2) values were calculated to be 0.73, 0.99, 0.99, 0.92, and 0.92 for AC, ALG, and AC-ALG-(1.0–3.0), respectively. According to R^2 values, Langmuir isotherm can be accepted as fitted well for tetracycline adsorption.

The Freundlich model (Eq. (3)) is applied to adsorption on heterogeneous surfaces.

$$q_e = K_F C_e^{1/n} \tag{3}$$

Table 1
Adsorption isotherm model parameters of tetracycline adsorption onto AC, ALG, and AC-ALG beads

	AC	ALG	AC-ALG-1.0	AC-ALG-2.0	AC-ALG-3.0
Langmuir isotherm model					
q_m (mg g^{-1})	8.4	0.1	0.4	62.5	13.7
K_L (L mg^{-1})	0.64	0.05	0.07	0.01	0.12
R_L	0.072	0.5	0.42	0.83	0.29
R^2	0.73	0.99	0.99	0.92	0.92
Freundlich isotherm model					
K_F (mg g^{-1})	3.53	110	221	12.1	1.9
$1/n$	0.387	17.2	1.0	10.9	0.6
R^2	0.96	0.96	0.92	0.94	0.96
D–R isothem model					
q_m (mg g^{-1})	–	–	–	8.8	8.2
β (mol^2 K J^{-2})	–	4×10^{-4}	1×10^{-4}	6×10^{-6}	2×10^{-6}
Energy (J mol^{-1})	–	35	70	280	500
R^2	0.56	0.96	0.93	0.78	0.75
Temkin isotherm model					
K_t (L g^{-1})	14.87	0.06	0.09	0.3	0.7
b (J mol^{-1})	945	70.3	47.3	414.5	620.2
R^2	0.83	0.87	0.93	0.99	0.98
Halsey isotherm model					
n_H	–0.38	–0.06	–0.09	–0.97	–1.60
K_H (mg g^{-1})	0.34	16	10	1.7	2.7
R^2	0.83	0.97	0.95	0.94	0.97
Harkins–Jura isotherm model					
A (g mg^{-1})	2.27	0.04	0.3	5.9	12.5
B (mg g^{-1})	0.13	1.23	1.11	1.19	1.23
R^2	0.94	0.98	0.98	0.99	0.97

where, K_F and $1/n$ represent the adsorption capacity and intensity, respectively. The value of $1/n$ represents the adsorption favorable condition [13,16,17].

The values of K_F and $1/n$ were calculated to be 3.53 mg g^{-1} and 0.387 for AC; 110 mg g^{-1} and 17.2 for ALG beads; 221 mg g^{-1} and 1.0 for AC-ALG-1.0 beads; 12.1 mg $g^{-1}$and 10.9 for AC-ALG-2.0; and 1.9 mg g^{-1} and 0.6 for AC-ALG-3.0 beads, as indicated in Table 1. It is clear that lower K_F values were found for higher AC contents. Furthermore, for tetracycline adsorption onto AC and AC-ALG-3.0 beads, $1/n$ value was lower than 1.0, so it can be safely mentioned that the Freundlich model was favorable for both AC and AC-ALG-3.0 beads. This result found that multilayer tetracycline adsorption onto heterogeneous AC and AC-ALG-3.0 surfaces was shown. The R^2 values of the model varied between 0.92 and 0.96 (Fig. 5, Table 1).

On the other hand, for tetracycline adsorption onto ALG, and AC-ALG-(1.0–2.0), $1/n$ values were higher than 1.0, so the Freundlich model was not favorable for tetracycline adsorption onto these beads. That is why it can be mentioned that tetracycline adsorption onto ALG, and AC-ALG-(1.0–2.0) beads can be characterized by the Langmuir model. According to the Langmuir model, it can be assumed that each active site of these beads interacted with only one tetracycline molecule; tetracycline molecules were adsorbed on well-defined localized sites, and the sites are energetically homogeneous. This situation can be explained in that when the amount of AC in the molecular structure of the ALG increases from 0.0% to 3.0%, the adsorption behavior shows the transition from the Langmuir model to the Freundlich model.

The D–R model (Eq. (4)) is based on heterogeneous adsorbent surfaces, adsorbent porosity, and adsorption free energy. The value of adsorption free energy gives information as to whether the adsorption process is physical or chemical in nature [9,13].

$$\ln q_e = \ln q_m - \beta(\varepsilon)^2 \tag{4}$$

where β ($mol^2\ kJ^{-2}$) and ε are model constants, R is universal gas constant, and T (K) is temperature. ε is equal to $RT\ln(1 + 1/C_e)$, which is the Polanyi potential. $q_{m,\text{calculated}}$ and β (Table 1) were calculated to be 8.8 mg g^{-1} and 6×10^{-6} $mol^2\ kJ^{-2}$; 8.2 mg g^{-1} and 2×10^{-6} $mol^2\ kJ^{-2}$ for AC-ALG-2.0 and AC-ALG-3.0 beads, respectively (Table 1). The coefficient of regression calculated between 0.75 and 0.96 for the D–R model. An adsorption process is called physical if the value of mean free energy is lower than 8 kJ mol^{-1}, and it is called chemisorption if the mean free energy values are between 8 and 16 kJ mol^{-1}. The mean free energies (equal to $1/(2\beta)^{1/2}$) were calculated to be 280 and 500 J mol^{-1} for AC-ALG-2.0 and AC-ALG-3.0 beads, which reflected that the chemisorption and tetracycline adsorption process onto all beads can be called physical.

The Temkin model (Eq. (5)) accepts that adsorption heat of all the molecules declines linearly as equilibrium adsorption capacity increases, and the adsorption is characterized by a uniform distribution of the binding energies.

$$q_e == \frac{RT\ln(K_t C_e)}{b} \tag{5}$$

where K_t (L g^{-1}) is model constant, b (J mol^{-1}) is the heat of adsorption constant, R is universal gas constant, and T (K) is temperature [13,17].

As shown in Table 1, K_t values were determined as 14.87, 0.09, 0.3, and 0.7 L g^{-1} for AC, AC-ALG-1.0, AC-ALG-2.0, and AC-ALG-3.0, respectively. Also, the heat of adsorption (b) values were calculated to be 945, 47.3, 414.5, and 620.2 J mol^{-1} for AC and AC-ALG-(1.0–3.0), respectively. Based on the R^2 values (0.83–0.99), the Temkin model fitted well to the equilibrium data.

The Halsey isotherm (Table 1) considers the multilayer adsorption onto a heterogeneous adsorbent surface and is defined with Eq. (6).

$$q_e = \frac{1}{n_H}\ln K_H - \frac{1}{n_H}\ln C_e \tag{6}$$

Where K_H and n_H are Halsey model constants [17].

Table 1 indicates the good fit for the adsorption data with high R^2 values between 0.83 and 0.97 for ALG and AC-ALG beads; this result confirmed multilayer tetracycline adsorption onto the heterogeneous surface of all beads. Moreover, the Freundlich model results also confirmed the applicability of this model.

The Harkins–Jura isotherm assumes multilayer adsorption occurring on an adsorbent surface having a heterogeneous pore distribution [13,17].

$$\frac{1}{q_e^2} = \frac{B}{A} - \left(\frac{1}{A}\right)\log C_e \tag{7}$$

In Eq. (7), A and B are model constants.

The values of constants A and B of the isotherm were calculated as 5.9 g mg^{-1} and 1.19 mg g^{-1}; 12.5 g mg^{-1} and 1.23 mg g^{-1} for AC-ALG-2.0 and AC-ALG-3.0, respectively (Fig. 5 and Table 1). This model showed better fitting to the adsorption data than the Langmuir, D–R, and Halsey models, with R^2 values in the range of 0.94 and 0.99.

According to the outcome of studying all models, the Langmuir and Freundlich models fitted to best for tetracycline adsorption onto AC-ALG-(1.0–2.0) beads and AC-ALG-3.0 beads, respectively. Tetracycline adsorption can be said to occur on monolayer AC-ALG-(1.0–2.0) bead surfaces. Furthermore, the Freundlich, D–R, Temkin, Halsey, and Harkins–Jura models fitted to the adsorption onto AC-ALG-3.0 beads, and tetracycline adsorption can be said to occur on multilayer heterogeneous AC-ALG-3.0 bead surfaces. The active sites of AC-ALG-3.0 beads increased logarithmically during the adsorption because of the occurring multilayer adsorption. It can be safely stated that the adsorption model passed from the Langmuir model to the Freundlich model, dopping a high amount of AC into the alginate structure due to the high surface area and pore size distribution of AC.

3.4. Adsorption kinetics

The effect of time of the tetracycline adsorption onto ALG and AC-ALG-(1.0–3.0) beads are represented in Fig. 6. The rate of tetracycline adsorption using AC-ALG beads was

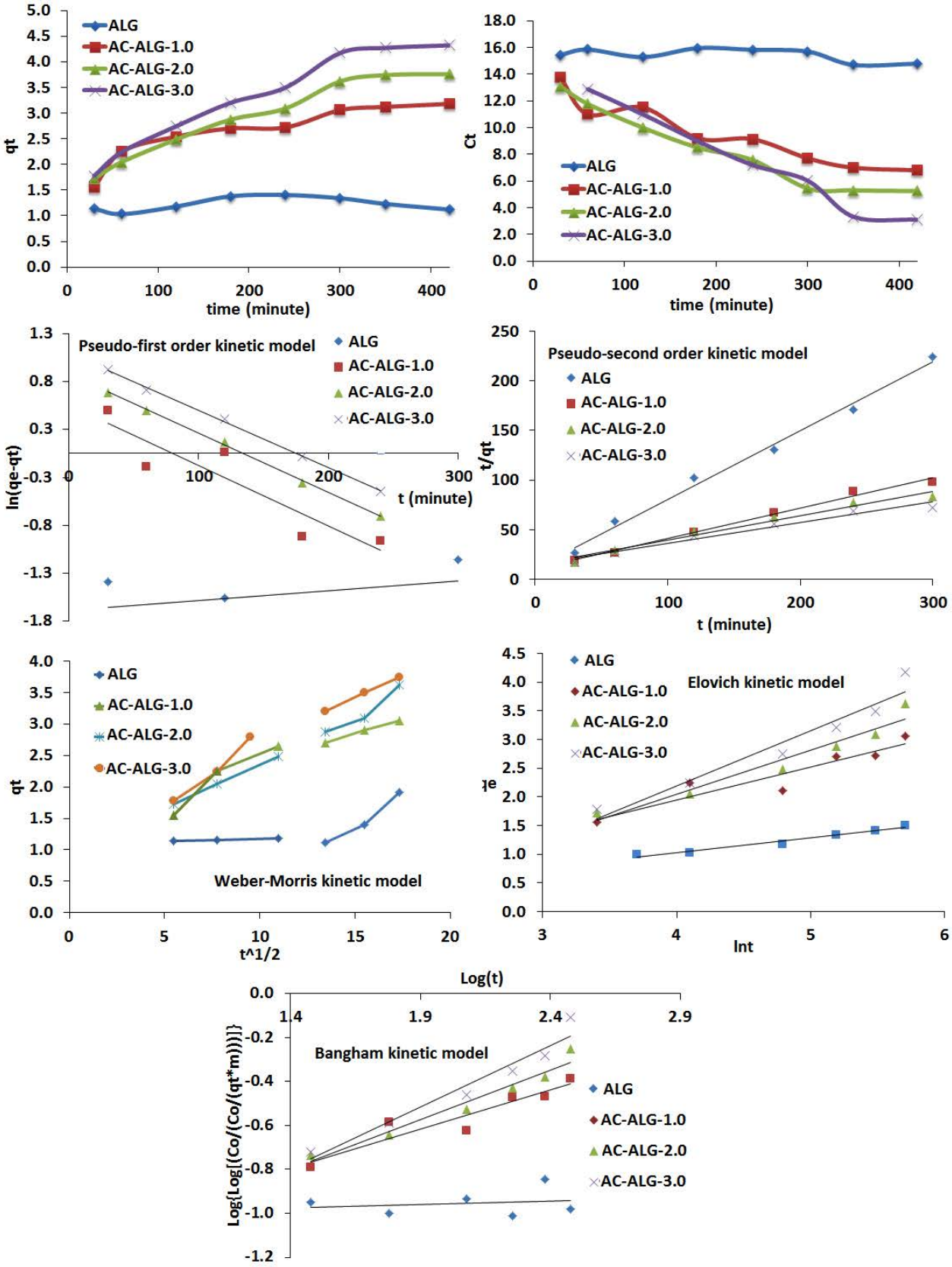

Fig. 6. Adsorption kinetic models of tetracycline onto ALG and AC-ALG beads.

very high during the first 4 h; then the adsorption continued at a slower rate and attained equilibrium at the end of 7 h. Tetracycline adsorption in the equilibrium conditions, C_t values of AC-ALG-(1.0–3.0) beads were found to be nearly 6.8, 5.6, and 3.1 mg L^{-1}, and q_t values were determined to be 3.2, 3.8, and 4.3 mg g^{-1}, respectively.

The adsorption kinetic models were characterized using pseudo-first-order, pseudo-second-order, Weber–Morris, Elovich, and Bangham models [18,19]. The pseudo-first-order model is a simple kinetic model and is expressed with Eq. (8).

$$\log\left(q_e - q_t\right) = \log q_e - \frac{k_1}{2.303}t \tag{8}$$

where k_1 (min^{-1}) is the rate constant of the model (Fig. 6 and Table 2).

In the present study, for the pseudo-first-order kinetic model, the experimental $q_{e,experimental}$ values were determined to be 3.2, 3.8, and 4.3 mg g^{-1} for AC-ALG-(1.0–3.0) beads, respectively. The $q_{e,calculated}$ values were calculated to be 3.0, 6.0, and 11.0 mg g^{-1} for the beads, and the R^2 values of AC-ALG beads varied between 0.84 and 0.99. $q_{e,calculated}$ values determined from the quietly different from $q_{e,experimental}$ values, and this result expressed the pseudo-first-order kinetic was not fitted for characterization of tetracycline adsorption.

The pseudo-second-order kinetic model assumes that the adsorption capacity is proportional to the number of active sites of the adsorbent and is defined with Eq. (9):

$$\frac{t}{q_t} = \frac{1}{k_2 q_e^2} + \frac{1}{q_e}t \tag{9}$$

where k_2 (g mg^{-1} min^{-1}) is the model constant, and it is initial sorption rate equal to $k_2 q_e^2$ [13,19].

For the pseudo-second-order kinetic, $q_{e,experimental}$ and $q_{e,calculated}$ values were nearly the same and determined to be $q_{e,experimental,AC\text{-}ALG\text{-}1.0}$ = 3.2 mg g^{-1} and $q_{e,calculated,AC\text{-}ALG\text{-}1.0}$ = 3.2 mg g^{-1}; $q_{e,experimental,AC\text{-}ALG\text{-}2.0}$ = 3.8 mg g^{-1}, and $q_{e,calculated,AC\text{-}ALG\text{-}2.0}$ = 4.04 mg g^{-1}; $q_{e,experimental,AC\text{-}ALG\text{-}3.0}$ = 4.3 mg g^{-1} and $q_{e,calculated,AC\text{-}ALG\text{-}3.0}$ = 4.7 mg g^{-1}. The initial adsorption rates were determined to be 0.1, 0.06, and 0.067 mg g^{-1} min^{-1} for AC-ALG-(1.0–3.0) beads, respectively. R^2 values were between 0.96 and 0.99 (Table 2). These results indicated that tetracycline adsorption onto all AC-ALG beads was characterized better by the pseudo-second-order kinetic than the pseudo-first-order kinetic model.

The Weber–Morris intraparticle diffusion model with multi-linearity correlations identifies the mass transfer

Table 2
Kinetic model parameters of tetracycline adsorption onto ALG and AC-ALG beads

	ALG	AC-ALG-1.0	AC-ALG-2.0	AC-ALG-3.0
q_e (mg g^{-1})	1.1	3.2	3.8	4.3
Pseudo-first-order kinetic model				
q_e (mg g^{-1})	42	3.0	6.0	11.0
k_1 (min^{-1})	0.023	0.014	0.014	0.014
R^2	0.10	0.84	0.99	0.99
Pseudo-second-order kinetic model				
q_e (mg g^{-1})	1.4	3.2	4.04	4.7
k_2 (g mg^{-1} min)	0.042	0.028	0.0041	0.003
h (mg g^{-1} min)	0.087	0.1	0.06	0.067
R^2	0.97	0.99	0.96	0.98
Weber–Morris intraparticle kinetic model				
k_{id1} (mg g^{-1} $min^{0.5}$)	0.0075	0.119	0.26	0.25
R^2	0.98	0.97	0.97	0.99
k_{id2} (mg g^{-1} $min^{0.5}$)	0.206	0.306	0.34	0.135
R^2	0.91	0.99	0.98	0.94
Elovich kinetic model				
β (g mg^{-1})	3.9	1.7	1.3	1.0
α (mg g^{-1} min)	0.3	1.0	1.6	1.7
R^2	0.10	0.85	0.98	0.98
Bangham kinetic model				
k_0 (L g^{-1})	0.0014	0.0007	0.0005	0.0004
α	0.0316	0.35	0.45	0.56
R^2	0.10	0.88	0.95	0.95

phenomena during the adsorption process, and the model is defined with Eq. (10):

$$q_t = k_{id} t^{0.5} + C \quad (10)$$

where k_{id} (mg g^{-1} min$^{-0.5}$) is the intraparticle rate constant [19].

The R^2 values for the model varied between 0.91 and 0.99, which was higher than the pseudo-second-order kinetic model. From Fig. 6 and Table 2, two separate linear stages with a different slope were determined for all beads, which can be identified as different mass transfer existing. The first phase in the first 2 h demonstrated the boundary layer transfer on the external surface of the beads. The second linear stage between three and 5 h described the intraparticle transfer [19,20].

where k_{id1} and k_{id2} values were determined as $k_{id1, ALG} = 0.0075$ and $k_{id2, ALG} = 0.206$ mg g^{-1} min$^{-0.5}$; $k_{id1, AC\text{-}ALG\text{-}1.0} = 0.119$ and $k_{id2, AC\text{-}ALG\text{-}1.0} = 0.306$ mg g^{-1}min$^{-0.5}$; $k_{id1, AC\text{-}ALG\text{-}3.0} = 0.25$ and $k_{id2, AC\text{-}ALG\text{-}3.0} = 0.135$ mg g^{-1}min$^{-0.5}$, respectively. The interior mass transfer rates were greater than that of the boundary layer for ALG and AC-ALG-1.0. The interior mass transfer rates were calculated as 27-fold and nearly three-fold higher than the boundary layer mass transfer rate for ALG and AC-ALG-1.0 beads, respectively.

The Elovich kinetic model expresses the heterogeneous systems for the adsorption process [20,21]. The model is defined as below:

$$q_t = \frac{1}{\beta}\ln(\alpha\beta) + \frac{1}{\beta}\ln t \quad (11)$$

where α (mg g^{-1} min^{-1}) and β (g mg^{-1}) are adsorption rate at $t = 0$ and desorption constant.

The correlation coefficients (R^2) of AC-ALG beads for the Elovich model varied to be between 0.85 and 0.98, and the initial adsorption rate (α) values were calculated as $\alpha_{AC\text{-}ALG\text{-}1.0} = 1.0$, $\alpha_{AC\text{-}ALG\text{-}2.0} = 1.6$, and $\alpha_{AC\text{-}ALG\text{-}3.0} = 1.7$ mg g^{-1} min^{-1}. It can be safely stated that the Elovich model was suitable for the characterization of the tetracycline adsorption (Table 2).

The Bangham equation is applied to check whether pore diffusion is a limiting step for the adsorption [19]. The model is expressed with Eq. (12).

$$\log\left[\log\left(\frac{C_0}{C_0 - q_t m}\right)\right] = \log\left(\frac{k_0 m}{2.303V}\right) + \alpha \log t \quad (12)$$

where k_0 (L g^{-1}) and α are Bangham model constants.

The R^2 values of AC-ALG beads were between 0.88 and 0.95 for the Bangham model (Fig. 6 and Table 2), so pore diffusion played an important role during the tetracycline adsorption.

3.5. Thermodynamic study

$\Delta H°$ values of tetracycline adsorption onto ALG and AC-ALG-(1.0–3.0) were calculated to be 121,713; 83,175; 86,507; and 92,839 J mol^{-1}, respectively, and this indicated that the tetracycline adsorption onto all beads was endothermic in nature [22,23]. The endothermic behavior of tetracycline adsorption was confirmed by the positive values of enthalpy, and positive/negative enthalpy values represented classify the chemical or physical adsorption (for chemical adsorption, $\Delta H° > 35{,}000$ J mol^{-1} and for physical adsorption $\Delta H° < 35{,}000$ J mol^{-1}) [24]. According to Table 3, the positive $\Delta H°$ values indicated tetracycline adsorptions onto AC dopped ALG beads were an endothermic reaction, so an increase of temperature supported the adsorption reaction. $\Delta S°$ values were determined as 359, 246, 282, and 317 J mol^{-1} K^{-1} for ALG, AC-ALG-(1.0–3.0), respectively, and the positive $\Delta S°$ values demonstrated that the disorderliness and conformational entropies of the beads and antibiotic interface increased during the adsorption process. The adsorption of tetracycline by AC-ALG-3.0 beads was spontaneous with the negative values of Gibbs free energy. The negative $\Delta G°$ values indicated that tetracycline adsorption was a spontaneous process and declined significantly with an increment in temperature representing spontaneous behavior of tetracycline removal process onto AC dopped alginate beads changed inversely with temperature.

3.6. Adsorption mechanism of tetracycline onto AC-ALG-3.0 beads

The chemical states of C and O species for AC-ALG-3.0 beads were performed using XPS before and after tetracycline adsorption (Fig. 7). From O 1s spectra of AC-ALG-3.0 beads, two main oxygen bands appeared at 532.93 and 531.34 eV, which represented C=O (acid or ester) bond, C=O states. The O 1s spectrum of tetracycline-adsorbed AC-ALG-3.0 beads showed a decrease at 532.93 eV from 67.34% to 44.3% due to the deformation of –COOH chemical states on the tetracycline and AC-ALG:3.0 beads. Furthermore, C 1s spectra of AC-ALG-3.0 beads showed five peaks with binding energies appointed at 286.52 (C–OH), 288.16 (COOH), 284.47 (C=C), 290.12 (π–π), and 285.3 (C–C and C–H), where C atom mainly occurred as

Table 3
Thermodynamic parameters of tetracycline adsorption onto ALG and AC-ALG beads

	ALG	AC-ALG-1.0	AC-ALG-2.0	AC-ALG-3.0
$\Delta H°$ (J mol^{-1})	121,713	83,175	86,507	92,839
$\Delta S°$ (J mol^{-1} K)	359	246	282	317
$\Delta G°$ (J mol^{-1}) at 298 K	14,597	9,741	2,351	–1,724
$\Delta G°$ (J mol^{-1}) at 313 K	7,408	4,812	–3,297	–8,071
$\Delta G°$ (J mol^{-1}) at 333 K	2,016	1,116	–7,533	–12,831

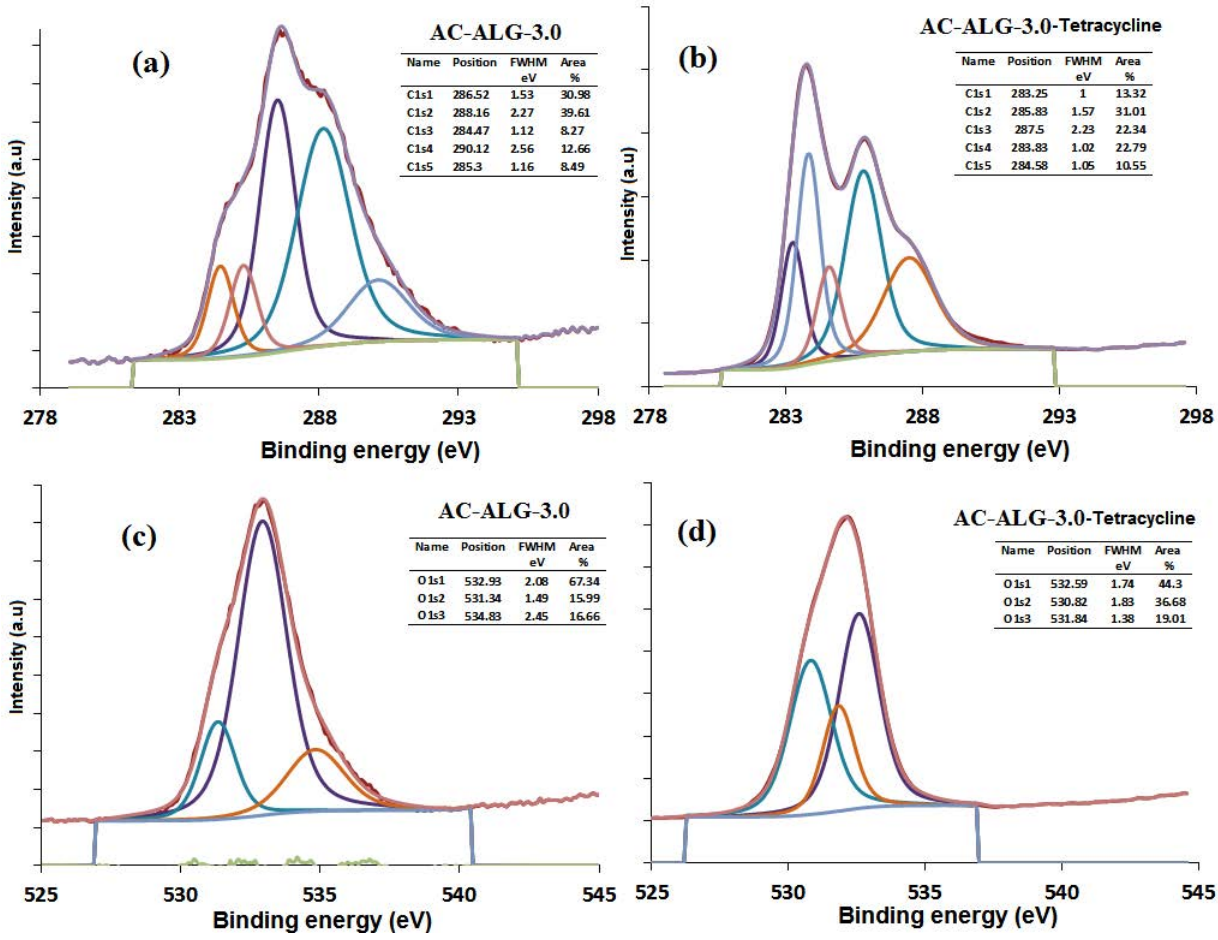

Fig. 7. XPS analysis of AC-ALG-3.0 beads before (a and c) and after tetracycline adsorption (b and d).

–COOH phase with the 39.61% atomic ratio. After tetracycline introducing on AC dopped ALG beads, –COOH state disappeared, due to –COOH bond of AC-ALG-3.0 beads and OH bond of tetracycline interacted. The ratio of C–C state (285.3 eV) increased from 8.49% to 31.01% (nearly 3.75-fold), and O–C–O (287.5 eV) new peak occurred, indicating that C–C and C–O groups played an important role for tetracycline adsorption.

Based on the C 1s and O 1s spectra, a plausible explanation for the tetracycline adsorption onto AC dopped ALG beads is shown in Fig. 8. The O–H, C–C, and O–C–O groups were responsible for tetracycline. The differences in the bands were evidence of interaction between tetracycline and AC-ALG-3.0 beads, and it can be safely mentioned that tetracycline was adsorbed on the AC-ALG-3.0 beads successfully.

3.7. Desorption and reusability of AC-ALG-3.0 beads

The desorption and reusability experiments are crucial for practical applications of adsorption, and it is an indicator of the performance of an adsorbent [25]. Therefore, AC-ALG-3.0 beads were subjected to desorption and reusability experiments. The loaded tetracycline was desorbed from the surface of AC-ALG:3.0 beads by NaOH, HCl, and ethanol to ensure that equilibrium was obtained. This experiment presents (Fig. 9a) that NaOH was able to desorb tetracycline from the beads with the highest efficiency in comparison with other solvents. The desorption percentages were found as 78%, 32%, and 48% when NaOH, HCl, and ethanol were used as desorption agents, respectively. Therefore, NaOH was selected as a desorption eluent phase in further experiments.

After selecting NaOH as a desorption eluent phase, adsorption experiments were performed until 10 cycles, and the results are shown in Fig. 9b. AC-ALG:3.0 beads were examined for reusability for 10 consecutive cycles. Almost 82% and 70% desorption efficiency was achieved using NaOH in the third and fourth cycles, respectively. The beads in the fifth consecutive cycles showed high performance, and the beads adsorbed nearly 58% of the tetracycline. It can be safely stated that no significant differences occurred in the adsorption capacity of the beads after the eighth cycle.

4. Comparison of adsorbents

A comparison of the maximum tetracycline removal percentages of different adsorbents with that of previously

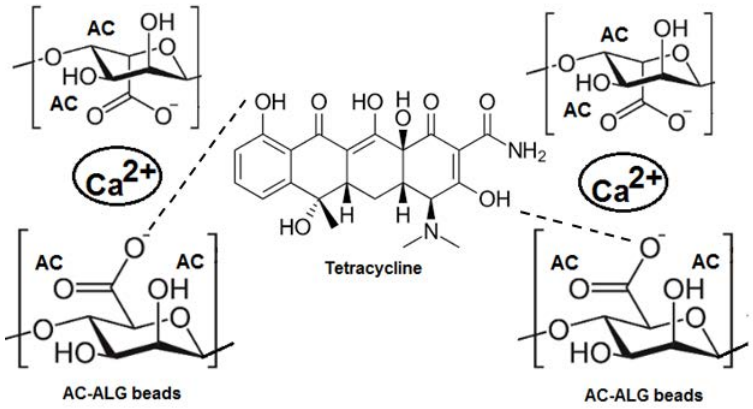

Fig. 8. Plausible tetracycline adsorption mechanism.

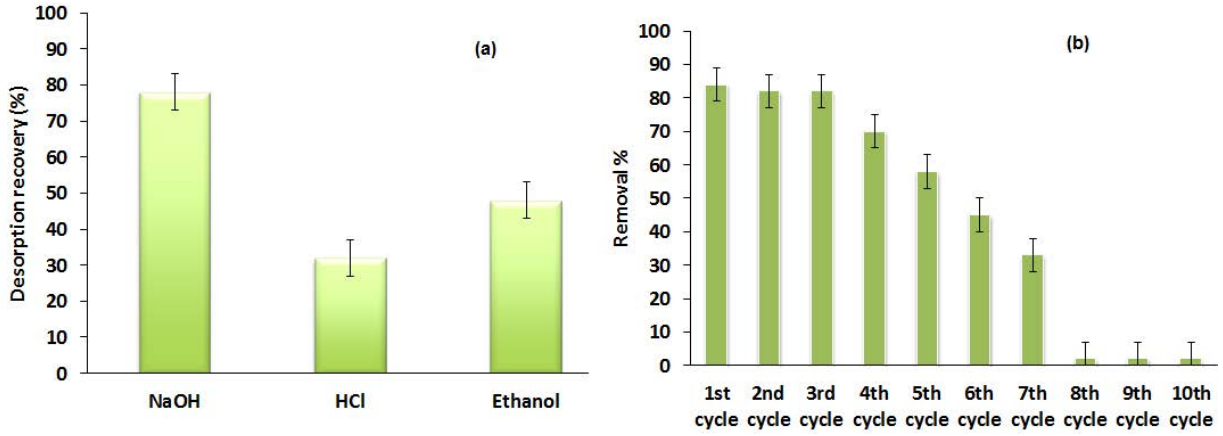

Fig. 9. (a and b) Desorption and reusability of AC-ALG-3.0 beads.

Table 4
Comparative evaluation of tetracycline adsorption removal % of similar adsorbents

Adsorbent	Tetracycline removal %	References
Hyacinth root	58.9	[26]
Hyacinth root	84.6	[26]
Granular sludge	93.1	[27]
Oxidized activated carbon	76.3	[28]
MCM-41-Zeolite	98.7	[29]
Aerobic granular sludge	90.0	[30]
Activated carbon dopped aginate beads	100	Present study

reported [26–30] adsorbents was investigated, and the results are represented in Table 4. The Table 4 shows that AC-ALG beads can be used effectively for the removal of tetracycline from wastewater.

5. Conclusion

Among various carbonaceous adsorbents used to remove antibiotics from wastewater, activated carbon is one of the most used sorbents due to its high surface area, pore size distribution, and adsorption capacity. Therefore, the highly porous structure and large specific surface area of activated carbon and the changeable properties and adsorption performance of alginate can be combined to prepare an efficient, new adsorbent for the adsorption of antibiotics from wastewater.

In this work, AC-ALG beads showed excellent adsorption capacities for tetracycline, with 100% removal in neutral

pH value, and could be easily separated and recycled using NaOH after the adsorption process. The adsorption isotherm models were well described by the Langmuir, Freundlich, Temkin, Halsey, and Harkins–Jura models for AC-ALG beads containing different amounts of AC, and adsorption executed a spontaneous and endothermic process. Furthermore, the experimental results illustrated that the adsorption of tetracycline was better shown by the pseudo-second-order model. The results from the present study represented that AC-ALG beads can serve as a new and innovative adsorbent for wastewaters for pharmaceutical compounds-polluted water purification.

Acknowledgment

The financial support provided by Yalova University Scientific Research Projects Coordination Department (Project no. 2018/YL/013) is gratefully acknowledged.

References

[1] S. Kim, P. Eichhorn, J.N. Jensen, A.S. Weber, D.S. Aga, Removal of antibiotics in wastewater: effect of hydraulic and solid retention times on the fate of tetracycline in the activated sludge process, Environ. Sci. Technol., 39 (2005) 5816–5823.
[2] A. Javid, A. Mesdaghinia, S. Nasseri, A.H. Mahvi, M. Alimohammadi, H. Gharibi, Assessment of tetracycline contamination in surface and groundwater resources proximal to animal farming houses in Tehran, Iran, J. Environ. Health Sci. Eng., 14 (2016) 1–5.
[3] H. Zhu, T. Chen, J. Liu, D. Li, Adsorption of tetracycline antibiotics from an aqueous solution onto graphene oxide/calcium alginate composite fibers, RSC Adv., 8 (2018) 2616–2621.
[4] K. Bedin, A. Martins, A. Cazetta, O. Osvaldo-Pezoti, V.C. Almeida, KOH-activated carbon prepared from sucrose spherical carbon: adsorption equilibrium, kinetic and thermodynamic studies for methylene blue removal, Chem. Eng. J., 286 (2016) 476–484.
[5] R. Torres-Caban, C.A. Vega-Olivencia, N. Mina-Camilde, Adsorption of Ni^{2+} and Cd^{2+} from water by calcium alginate/spent coffee grounds composite beads, Appl. Sci., 9 (2019) 4531–5452.
[6] H. Daemi, M. Barikami, Synthesis and characterization of calcium alginate nanoparticles, sodium homopolymannuronate salt and its calcium nanoparticles, Sci. Iran., 19 (2012) 2023–2028.
[7] H. Saygılı, F. Guzel, Effective removal of tetracycline from aqueous solution using activated carbon prepared from tomato (*Lycopersicon esculentum* mill.) industrial processing waste, Ecotoxicol. Environ. Saf., 131 (2016) 22–29.
[8] D. Saloglu, N. Ozcan, Activated carbon embedded chitosan/polyvinyl alcohol biocomposites for adsorption of nonsteroidal anti-inflammatory drug-naproxen from wastewater, Desal. Water Treat., 107 (2018) 72–84.
[9] E. Bilgin Simsek, D. Saloglu, N. Ozcan, I. Novak, D. Berek, Carbon fiber embedded chitosan/PVA composites for decontamination of endocrine disruptor bisphenol-A from water, J. Taiwan Inst. Chem. Eng., 70 (2017) 291–301.
[10] P.H. Chang, Z. Li, J.S. Jean, W.T. Jiang, Q. Wu, C.Y. Kuo, J. Kraus, Desorption of tetracycline from montmorillonite by aluminum, calcium, and sodium: an indication of intercalation stability, Int. J. Environ. Sci. Technol., 11 (2014) 633–644.
[11] A. Saarai, V. Kasparkova, T. Sedlacek, P. Saha, On the development and characterization of crosslinked sodium alginate/gelatine hydrogels, J. Mech. Behav. Biomed. Mater., 18 (2013) 152–166.
[12] C. Saka, BET, TG–DTG, FT-IR, SEM, iodine number analysis and preparation of activated carbon from acorn shell by chemical activation with $ZnCl_2$, J. Anal. Appl. Pyrolysis, 95 (2012) 21–24.
[13] O.I. Sahin, B. Yalcin, D. Saloglu, Adsorption of ibuprofen from wastewater using activated carbon and graphene oxide embedded chitosan–PVA: equilibrium, kinetics, and thermodynamics and optimization with central composite design, Desal. Water Treat., 179 (2020) 396–417.
[14] S. Yapar, V. Ozbudak, A. Dias, A. Lopes, Effect of adsorbent concentration to the adsorption of phenol on hexadecyl trimethyl ammonium-bentonite, J. Hazard. Mater., 121 (2005) 135–139.
[15] H.Y. Tran, S.J. You, A.H. Bandegharaei, H.P. Chao, Mistakes and inconsistencies regarding adsorption of contaminants from aqueous solutions: a critical review, Water Res., 120 (2017) 88–116.
[16] N. Ayawei, A.N. Ebelegi, D. Wankasi, Modelling and interpretation of adsorption isotherms, J. Chem., 2017 (2017) 1–12.
[17] A.A. Inyinbor, F.A. Adekola, G.A. Olatunji, Kinetics, isotherms and thermodynamic modeling of liquid phase adsorption of rhodamine b dye onto *raphia hookerie* fruit epicarp, Water Resour. Ind., 15 (2016) 14–27.
[18] S. Gholitabar, H. Tahermansouri, Kinetic and multi-parameter isotherm studies of picric acid removal from aqueous solutions by carboxylated multi-walled carbon nanotubes in the presence and absence of ultrasound, Carbon Lett., 22 (2017) 14–24.
[19] G. Vijayakumar, R. Tamilarasan, M. Dharmendirakumar, Adsorption, kinetic, equilibrium and thermodynamic studies on the removal of basic dye rhodamine-B from aqueous solution by the use of natural adsorbent perlite, J. Mater. Environ. Sci., 3 (2012) 157–170.
[20] M. Zhang, H. Zhang, D. Xu, L. Han, D. Niu, B. Tian, J. Zhang, L. Zhang, W. Wu, Removal of ammonium from aqueous solutions using zeolite synthesized from fly ash by a fusion method, Desalination, 271 (2011) 111–121.
[21] L. Largitte, R. Pasquier, A review of the kinetics adsorption models and their application to the adsorption of lead by an activated carbon, Chem. Eng. Res. Des., 109 (2016) 495–504.
[22] Y. Liu, Y.J. Liu, Biosorption isotherms, kinetics and thermodynamics, Sep. Purif. Technol., 61 (2008) 229–242.
[23] B.H. Yener, Removal of cefdinir from aqueous solution using nanostructure adsorbents of TiO_2, SiO_2 and TiO_2/SiO_2: equilibrium, thermodynamic and kinetic studies, Chem. Biochem. Eng. Q., 33 (2019) 235–248.
[24] Q. Zhu, G.D. Moggridge, C. D'Agostino, Adsorption of pyridine from aqueous solutions by polymeric adsorbents MN 200 and MN 500. Part 2: kinetics and diffusion analysis, Chem. Eng. J., 306 (2016) 1223–1233.
[25] M.H. Zarghi, A. Roudbari, S. Jorfi, N. Jaafarzadehc, Removal of estrogen hormones (17b-estradiol and estrone) from aqueous solutions using rice husk silica, Chem. Biochem. Eng. Q., 33 (2019) 281–293.
[26] X. Liu, B. Tang, Q. Zhang, L. Liu, R. Fan, Z. Zhang, The presence of Cu facilitates adsorption of tetracycline (TC) onto water hyacinth roots, Int. J. Environ. Res. Public Health, 15 (2018) 1982–1997.
[27] K. Li, F. Ji, Y. Liu, Z. Tong, X. Zhan, Z. Hu, Adsorption removal of tetracycline from aqueous solution by anaerobic granular sludge: equilibrium and kinetic studies, Water Sci. Technol., 67 (2013) 1490–1496.
[28] Q. Qin, X. Wu, L. Chen, Z. Jiang, Y. Xu, Simultaneous removal of tetracycline and Cu(II) by adsorption and coadsorption using oxidized activated carbon, RSC Adv., 8 (2018) 1744–1452.
[29] Y. Guo, W. Huang, B. Chen, Y. Zhao, D. Liu, Y. Sun, B. Gong, Removal of tetracycline from aqueous solution by MCM-41-zeolite A loaded nano zero valent iron: synthesis, characteristic, adsorption performance and mechanism, J. Hazard. Mater., 339 (2017) 22–32.
[30] X. Wang, Z. Chen, J. King, Z. Zhao, J. Shen, Removal of tetracycline by aerobic granular sludge and its bacterial community dynamics in SBR, RSC Adv., 8 (2018) 18284–18293.

Supplementary information

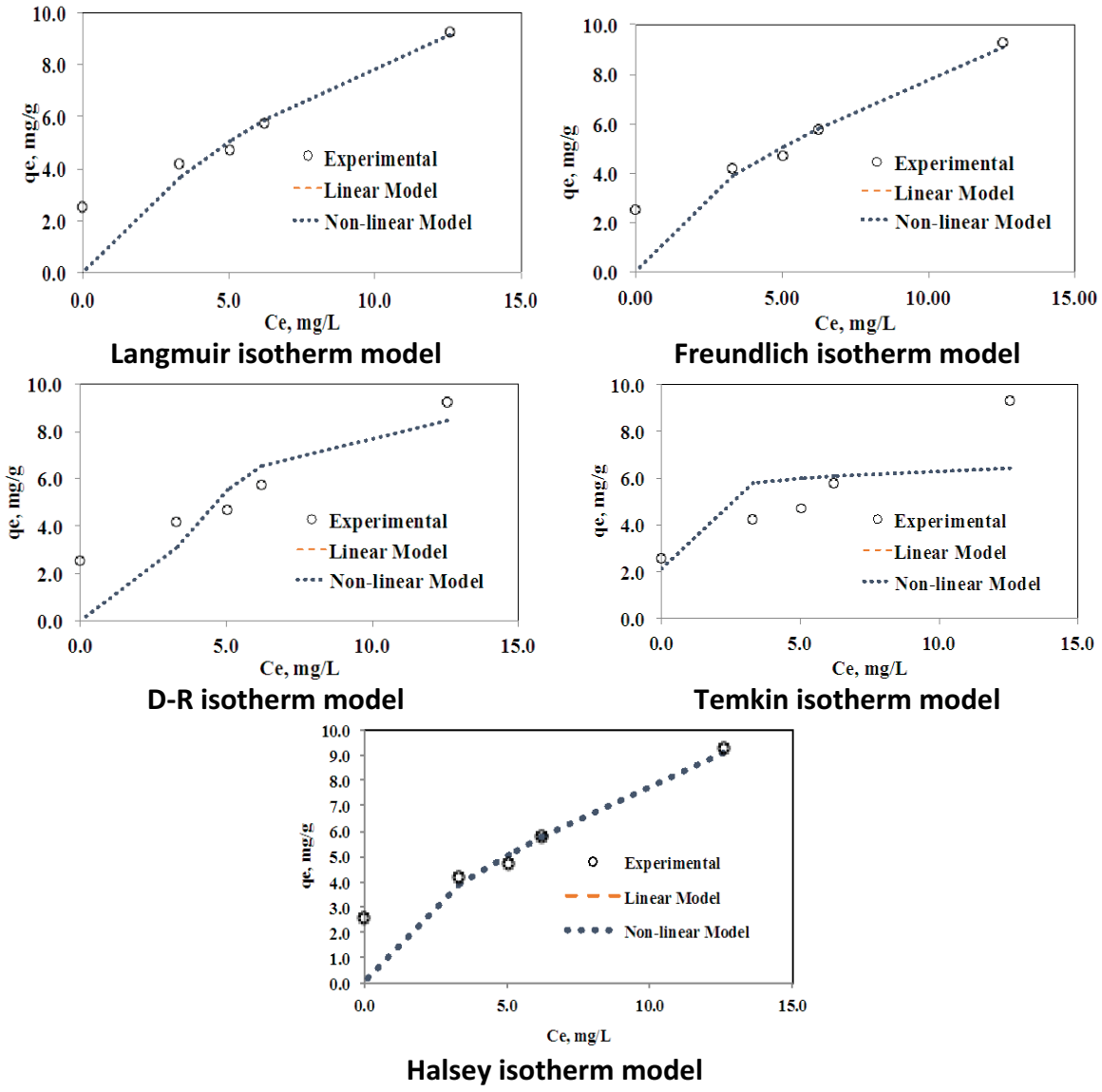

Fig. S1. Comparison of the isotherm model capacities of AC-ALG-3.0 beads.

Table S1
Comparison of R^2 and X^2 values of AC-ALG-3.0 beads

Model	R^2 (From Table 1)	X^2
Langmuir model	0.96	0.11
Freundlich model	0.92	0.05
D–R model	0.75	1.64
Temkin model	0.98	0.67
Halsey model	0.97	0.05